Cell, Vol. 109, 811–821, June 28, 2002, Copyright ©2002 by Cell Press

Unrepaired DNA Breaks in p53-Deficient Cells Lead to Oncogenic Gene Amplification Subsequent to Translocations

Chengming Zhu,[1,7] Kevin D. Mills,[1,7] David O. Ferguson,[1,2,4,7] Charles Lee,[2,4] John Manis,[1] James Fleming,[1] Yijie Gao,[1] Cynthia C. Morton,[2,4,5] and Frederick W. Alt[1,3,6]

[1]Howard Hughes Medical Institute
The Children's Hospital and The Center for Blood Research
Boston, Massachusetts 02115
[2]Department of Pathology
[3]Department of Genetics
Harvard University Medical School
Boston, Massachusetts 02115
[4]Department of Pathology
[5]Department of Obstetrics, Gynecology, and Reproductive Biology
Brigham and Women's Hospital
Boston, Massachusetts 02115

Summary

Amplification of large genomic regions associated with complex translocations (complicons) is a basis for tumor progression and drug resistance. We show that pro-B lymphomas in mice deficient for both p53 and nonhomologous end-joining (NHEJ) contain complicons that coamplify *c-myc* (chromosome 15) and IgH (chromosome 12) sequences. While all carry a translocated (12;15) chromosome, coamplified sequences are located within a separate complicon that often involves a third chromosome. Complicon formation is initiated by recombination of RAG1/2-catalyzed IgH locus double-strand breaks with sequences downstream of *c-myc*, generating a dicentric (15;12) chromosome as an amplification intermediate. This recombination event employs a microhomology-based end-joining repair pathway, as opposed to classic NHEJ or homologous recombination. These findings suggest a general model for oncogenic complicon formation.

Introduction

A hallmark of tumorigenesis is genomic instability, which manifests as chromosomal aberrations such as translocations and amplifications (reviewed in Lengauer et al., 1998). While these changes can be simple, such as balanced reciprocal translocations or localized gene amplification, many involve complex unbalanced translocations associated with amplification of sizable regions. The latter events, which we refer to collectively as complicons, have been noted in association with pathogenesis and progression of various solid and disseminated cancers (Coene et al., 1997; Padilla-Nash et al., 2001). Complicons can also be associated with the acquisition of resistance to chemotherapeutic agents in vitro (Federspiel et al., 1984) and in vivo (Gorre et al., 2001). Molecular mechanisms that generate complicons are poorly understood, due partly to their inherent complexity and diversity, as well as lack of experimental models to track progression from initiation to final outcome.

The classic nonhomologous end-joining (NHEJ) pathway of DNA double-strand break repair (DSBR) is critical for maintaining genome stability (reviewed in Ferguson and Alt, 2001). Known NHEJ factors include Ku70, Ku80, DNA-PK catalytic subunit (DNA-PKcs), Artemis, XRCC4, and DNA ligase IV (Lig4) (reviewed in Bassing et al., 2002). NHEJ is required in developing lymphocytes for assembly of antigen receptor variable region genes from component V, D, and J gene segments. This V(D)J recombination process is initiated by the site-specific RAG1/2 endonuclease, which introduces DNA double-strand breaks (DSB) between participating gene segments and flanking recombination signal sequences (RSSs) (Fugmann et al., 2000). Subsequently, V(D)J recombination is completed via repair of resultant DSBs by NHEJ. Deficiency for any NHEJ factor results in a substantial defect in V(D)J coding joint formation, and thus a severe combined immunodeficiency (SCID) (reviewed in Bassing et al., 2002).

Mice deficient for XRCC4, Lig4, or Ku also suffer extensive apoptosis of developing neurons, with XRCC4$^{-/-}$ and DNA Lig4$^{-/-}$ mice exhibiting late embryonic lethality (Frank et al., 1998; Gao et al., 1998; Gu et al., 1997). In these mice, neuronal apoptosis and embryonic lethality are dramatically rescued by homozygous inactivation of the p53 tumor suppressor gene (Frank et al., 2000; Gao et al., 2000). However, lymphocyte development is not rescued, because p53 and NHEJ-deficient prolymphocytes still cannot properly join V(D)J segments. Despite survival to adulthood, rescued XRCC4$^{-/-}$,p53$^{-/-}$ or Lig4$^{-/-}$,p53$^{-/-}$ (hereafter referred to as X/P and L/P, respectively) mice, as well as those doubly deficient for Ku80 (or DNA-PKcs) and p53, routinely succumb to pro-B cell lymphomas between 6 and 16 weeks after birth (Difilippantonio et al., 2000; Frank et al., 2000; Gao et al., 2000; Lim et al., 2000; Vanasse et al., 1999). The X/P and L/P lymphomas universally harbor an unbalanced, nonreciprocal translocation containing a distal portion of chromosome 15 fused to the majority of chromosome 12, der(12)t(12;15), which we hereafter refer to as C12;15 (with C identifying the derivative chromosome containing the centromere). Moreover, the X/P and L/P lymphomas, as well as the Ku80$^{-/-}$,p53$^{-/-}$ lymphomas, contain substantial amplification of both *c-myc* and segments of the IgH locus. The chromosomal alterations in these tumors were noted to be reminiscent of those in human Burkitt's lymphomas (Difilippantonio et al., 2000). However, the relationship between the recurrent chromosome 12 and 15 translocations and *c-myc*/IgH amplification is unknown.

Gene amplification generally refers to an increased dosage of a gene or genomic region. Mammalian gene amplification was discovered as the mechanism underlying overproduction of dihydrofolate reductase in methotrexate-resistant mammalian cells (Alt et al., 1978). Subsequent studies revealed amplification both as a

[6]Correspondence: alt@rascal.med.harvard.edu
[7]These authors contributed equally to this work.

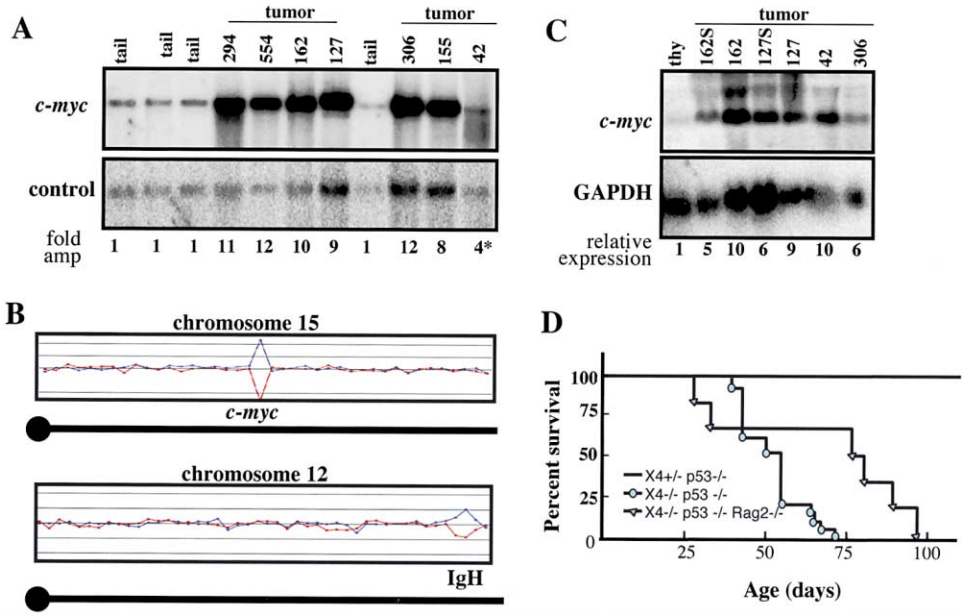

Figure 1. X/P and L/P Mice Exhibit Amplified IgH and *c-myc* Loci with Overexpression of the *c-myc* Gene

(A) Southern blot analysis of tumor samples and controls (tail DNA from normal mice). Fold amplification of *c-myc* is indicated below each lane and is shown relative to control lanes and normalized for loading (control probe, fragment of the LR8 gene detecting a 14 kb genomic fragment). Asterisk: DNA from tumor #42 was partially degraded, the fold of amplification is possibly underestimated. Amplification at the IgH and *c-myc* regions is confirmed by array CGH data (see Supplemental Data at http://www.cell.com/cgi/content/full/109/7/811/DC1).

(B) A typical array-CGH profile from tumor #155. Blue trace indicates the ratio of the test to reference hybridization signal. Red indicates the ratio of the reference to test. Symmetric blue over red peaks indicate amplified regions.

(C) Northern blot of tissue from normal mice and tumor samples is shown with loading control (GAPDH probe). Expression level of c-*myc* is indicated relative to the expression level in normal thymus normalized for loading (control probe, GAPDH).

(D) Survival curves for XRCC4$^{+/-}$ p53$^{-/-}$, XRCC4$^{-/-}$ p53$^{-/-}$, and RAG2$^{-/-}$ XRCC4$^{-/-}$ p53$^{-/-}$ mice. Percent survival is indicated as a function of age. (X4$^{+/-}$ p53 $^{-/-}$ [n = 8]; X4$^{-/-}$ p53 $^{-/-}$ [n = 12]; R2$^{-/-}$ X4$^{-/-}$ p53$^{-/-}$ [n = 6]).

common mechanism for anticancer drug resistance, and also as a characteristic of an ever-increasing number of human tumors (reviewed in Kuehl and Bergsagel, 2002; Schwab, 1999). In the latter context, amplification commonly results in overexpression of cellular oncogenes and has been implicated in several stages of tumor development (Lengauer et al., 1998). Studies of acquired drug resistance in transformed cell lines have led to the articulation of several different models for gene amplification. Broadly, these models include unequal sister chromatid exchange, extrachromosomal amplification and reintegration, localized overreplication, and breakage-fusion-bridge cycles (reviewed in Stark, 1993).

Cytogenetic evidence suggested that DNA breakage could play a key role in amplification (Windle et al., 1991). In this regard, drug resistance studies showed that amplification rates can be increased by ionizing radiation (Paulson et al., 1998) or clastogenic compounds (Kuo et al., 1994; Livingstone et al., 1992; Paulson et al., 1998), as well as by proximity to chromosome fragile sites (Coquelle et al., 1997) or DSBs (Pipiras et al., 1998). Various studies also suggested that DNA breakage could initiate a classic breakage fusion bridge (BFB) mechanism (McClintock, 1941), in which broken sister chromatids would fuse at their termini to generate dicentrics that could reenter the BFB cycle (Ma et al., 1993; Smith et al., 1990; Toledo et al., 1992). Other studies showed that p53 suppresses amplification in the context of drug resistance (Livingstone et al., 1992; Yin et al., 1992). In this regard, p53 deficiency was suggested to allow cells to move inappropriately into S phase and acquire DSBs that initiate amplification (Paulson et al., 1998). On the other hand, it also is conceivable that checkpoint deficiencies allow replication of preexisting DSBs, thus creating chromatid substrates for BFB amplification.

In contrast to standard amplification in drug-resistant cells, little is known about the mechanism of complicon formation in the context of cytogenetic tumor progression. Herein, we report that X/P and L/P mice reproducibly succumb to pro-B cell lymphomas that feature complicons harboring coamplified *c-myc* and IgH sequences. In addition, we elucidate, in detail, the molecular mechanism by which these complicons arise.

Results

Amplification and Overexpression of *c-myc* in L/P or X/P Pro-B Cell Lymphomas

X/P mice and L/P mice reproducibly develop pro-B cell lymphomas that contain a C12;15 translocation and show genomic coamplification of the cellular protooncogene *c-myc* and IgH sequences. We exploited this system to study molecular mechanisms of gene amplification leading to tumorigenesis. We have analyzed a total of 20 L/P or X/P mice. All doubly deficient animals were smaller than wild-type littermates and developed tumors

between 6 and 12 weeks after birth. All tumors were B220-positive and negative for surface IgM expression (data not shown and Frank et al., 2000; Gao et al., 2000), confirming pro-B lymphocyte origin.

To assay for *c-myc* amplification, tumor DNA was analyzed by Southern blotting for hybridization with a promoter-proximal *c-myc* probe. All but two of 20 analyzed X/P or L/P pro-B lymphomas showed substantial amplification (Figure 1A; see Supplemental Data at http://www.cell.com/cgi/content/full/109/7/811/DC1; Frank et al., 2000; Gao et al., 2000). Significantly, the two tumors with no (#184) or, at most, modest (#146) *c-myc* amplification appeared distinguishable from the others based on the nature of their translocations (see below). All pro-B cell tumors also contained discrete IgH locus rearrangements. Of these, most contained an amplified J_H allele (see Supplemental Data; Frank et al., 2000; Gao et al., 2000), suggesting that amplified translocation breakpoints may occur within the J_H region. As J_H rearrangements in X/P or L/P progenitor B cells can lead to deletion of the J_H locus (Frank et al., 2000; Gao et al., 2000), we also assayed tumor DNAs for hybridization to downstream IgH probes. Significantly, all 18 lymphomas that clearly contained *c-myc* amplification also had IgH locus amplification, as demonstrated by an HS3a enhancer probe (see Supplemental Data). The latter element derives from the 3′ IgH regulatory region (IgH3′RR) 200 kb downstream from the J_H locus (Manis et al., 2002).

To examine the specificity of the IgH and *c-myc* amplification, we surveyed the entire genome of selected tumors for additional amplifications and deletions via array-based comparative genomic hybridization (array-CGH) (Pinkel et al., 1998; Sharpless et al., 2001). Array-CGH detects amplification and deletion by simultaneous comparative hybridization to a genomic BAC array with normal control DNA and experimental sample DNA. Four tumors (#155, #42, #171, and #306), with evidence of significant IgH/*c-myc* amplification based on Southern blotting, were analyzed by array-CGH. Of these, three of four showed substantial amplification of a distal region on chromosome 12, in the vicinity of the J_H locus (Figure 1B; see Supplemental Data at http://www.cell.com/cgi/content/full/109/7/811/DC1). IgH locus amplification as judged by Southern blotting in the single tumor (#306) that did not show chromosome 12 amplification by array-CGH suggests that the amplified segment of chromosome 12 in this tumor was below the 3 megabase pair resolution of the array-CGH assay. Additionally, all four assayed tumors showed amplification of a medial region of chromosome 15, in the vicinity of the *c-myc* gene (Figure 1B; see Supplemental Data). The only other definitive amplification detected by array-CGH occurred in tumor #155 and involved a portion of chromosome 14 spanning the TCRα locus, a result confirmed by Southern blotting (data not shown). In addition to *c-myc* and IgH locus amplification, the array CGH analyses suggested a possible recurrent deletion within chromosome 9 (see Supplemental Data).

Deregulation of *c-myc* expression often appears to play a crucial role in malignant transformation of human B lineage cells. Thus, we assayed for *c-myc* transcripts in X/P and L/P tumors via Northern blotting with a probe specific for the first and second *c-myc* exons. These analyses revealed that *c-myc* transcript levels in four different tumors analyzed were substantially greater than levels in a normal adult thymus (Figure 1C), the normal tissue that exhibits highest *c-myc* expression (Zimmerman and Alt, 1990).

Requirement for RAG in Pro-B Lymphomagenesis in X/P Mice

The C12;15 and associated IgH and *c-myc* amplification in X/P and L/P pro-B cell tumors suggested that the translocation/amplification process may involve RAG-initiated DSBs (Frank et al., 2000; Gao et al., 2000). We tested this directly by examining triple mutant mice deficient for RAG2, p53, and XRCC4, which were obtained as offspring from parents that were XRCC4$^{+/-}$, p53$^{-/-}$ (or p53$^{+/-}$), and RAG$^{-/-}$ (or RAG$^{+/-}$). Six XRCC4$^{-/-}$, p53$^{-/-}$, RAG$^{-/-}$ mice were obtained, and all were approximately 50% the size of XRCC4$^{+/-}$ or XRCC4$^{+/+}$ littermates, as previously reported for p53-rescued Lig4- or XRCC4-deficient mice (Frank et al., 2000; Gao et al., 2000). Two triple mutant mice died early from unknown causes other than pro-B lymphoma, and four others were sacrificed when moribund between 78 and 97 days of age (Figure 1D). Median survival time for these mice appeared longer than that of X/P mice ($p < 0.1$). More importantly, necropsy of four mice and complete histologic analysis of one revealed no anatomic or microscopic evidence of lymphoma, in striking contrast to X/P mice which nearly all developed lymphomas ($p < 0.01$). In fact, no abnormal masses were identified, rendering an exact cause of death difficult to determine, although histology revealed a wide variety of degenerative anomalies in multiple organ systems, as well as two microscopic medulloblastomas (D.O.F., Y.G., and F.W.A., unpublished data). However, given the complexities in generating triple mutant mice, the significance of the latter findings await analyses of p53-deficient, conditional NHEJ-deficient mice. Overall, our results clearly demonstrate that occurrence of X/P pro-B lymphomas requires integrity of the RAG2 gene.

Complex Translocations Associated with Amplification

Because X/P and L/P mice exhibit significant genomic instability, even in some nontransformed cells (reviewed in Ferguson and Alt, 2001), genomic rearrangements other than C12;15 may occur in X/P or L/P lymphomas. To assay for additional chromosomal aberrations, we performed spectral karyotyping (SKY) (Liyanage et al., 1996) on metaphases from 8 L/P tumor-derived cell cultures. SKY confirmed the presence of a C12;15 translocation in all (e.g., Figures 2A and 2C; representative data), with nearly 100% of the metaphases exhibiting this translocation in most tumors. In addition to the C12;15, SKY also revealed the presence of complex translocations harboring portions of chromosomes 12 and 15. Most often, these structures involved chromosome 12- and 15-derived material fused to material from a third chromosome. For example, a tripartite translocation, der(15)t(12;15)t(6;12), containing the centromere of chromosome 15 attached to chromosome 12 material and terminating with chromosome 6 material (denoted as C15;12;6), was observed in tumor #162 (Figure 2A).

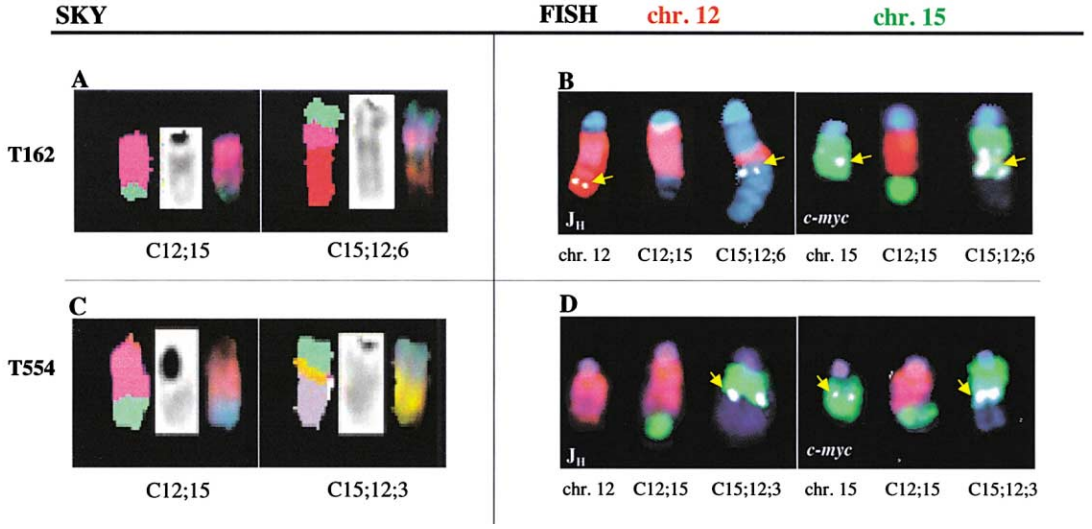

Figure 2. X/P and L/P Lymphomas Harbor Complicons Containing Coamplified *c-myc* and IgH

(A and C) Spectral karyotype (SKY) analysis of tumors #162 (A) and #554 (C).

(B and D). Fluorescence in situ hybridization (FISH) with locus-specific probes and chromosome paints of tumors #162 (B) and #554 (D). Chromosome 12 is red, chromosome 15 is green. Locus-specific signals are white (yellow arrows); IgH, left; *c-myc*, right. All chromosomes are counterstained with DAPI (blue).

Other examples include a C15;12;3 in tumor 554 (Figure 2C) and a C15;12;14 in tumor R3 (see Supplemental Data at http://www.cell.com/cgi/content/full/109/7/811/DC1). In another tumor (#127), chromosome 12- and 15-derived material were located on a chromosome 6 derivative, generating a C6;15;12;6, while in yet another tumor (#155), there was a C12;15 as well as C12;14 and C14;12 translocations likely related to the amplification of chromosome 14 TCRα locus sequences (see Supplemental Data).

Previous FISH data demonstrated coamplification of IgH and *c-myc* in NHEJ/p53 double null pro-B lymphoma cells (Difilippantonio et al., 2000; Gao et al., 2000). While it seemed likely that the amplified sequences might be on the recurrent C12;15, these studies did not reveal the amplicon location. For this purpose, FISH analyses were performed using probes specific to the *c-myc* and IgH loci, in conjunction with whole-chromosome paints specific for chromosomes 12 and 15. Surprisingly, these studies revealed that the amplified *c-myc* and IgH sequences were associated with complex translocations and not with the C12;15 (Figures 2B and 2D and data not shown). For example, in tumors #162 and #554, coamplified IgH/*c-myc* sequences were located on the complex derivative chromosome 15 (Figures 2B and 2D), and in tumor #127 the coamplified IgH/*c-myc* was on the chromosome 6 derivative (data not shown).

None of the tumors analyzed routinely contained even single-copy IgH or *c-myc* sequences on the C12;15 (e.g., Figures 2B and 2D), although a subset of tumor #127 metaphases contained apparently low or single-copy IgH and *c-myc* on a C12;15 and a C15;12 (data not shown). As neither the C15;12- nor the C12;15-containing *c-myc* were observed in any other tumors, we speculate these translocations may represent complicon-related by-products and/or independent translocation events in tumor #127. To further characterize the recurrent C12;15 translocations, we performed FISH analyses with a telomere-15-proximal probe; these analyses indicated that the C12;15, while lacking *c-myc* (except in a subset of tumor #127 metaphases), harbored the telomere-proximal region of chromosome 15, indicating that it generally derived from chromosome 15 regions downstream of the *c-myc* gene (see below and data not shown). In summary, *c-myc* and IgH were coamplified and associated with a complex translocation product that usually was either (1) derived from chromosome 15 and terminated with material from a third, nonhomologous chromosome, or (2) derived from a third chromosome but contained coamplified IgH/*c-myc* embedded within the translocation product. In addition, IgH and *c-myc* loci were generally absent from the clear-cut C12;15.

Microhomology at the Translocation Junctions

The recombination pathway that leads to chromosomal translocations in the absence of NHEJ is unknown. One possibility is homologous recombination (HR). Alternatively, RAG may promote transchromosomal recombination. A potential molecular footprint of such pathways would be DNA homology tracts or cryptic RSSs at or near translocation junctions. Breakpoint sequences from nine separate translocation junctions were analyzed and mapped to the single nucleotide level. In all cases, translocation junctions contained very short (1–6 nucleotides) sequence homologies (Figure 3A), suggesting involvement of an end-joining pathway, still not well characterized, that employs such short homologies (Roth and Wilson, 1986). There was no apparent nucleotide addition at any of these junctions. Germline sequences surrounding chromosome 12 and 15 breakpoints contained no significant sequence homologies. Likewise, no obvious RSSs were found in the sequences closely flanking the chromosome 15 breakpoints.

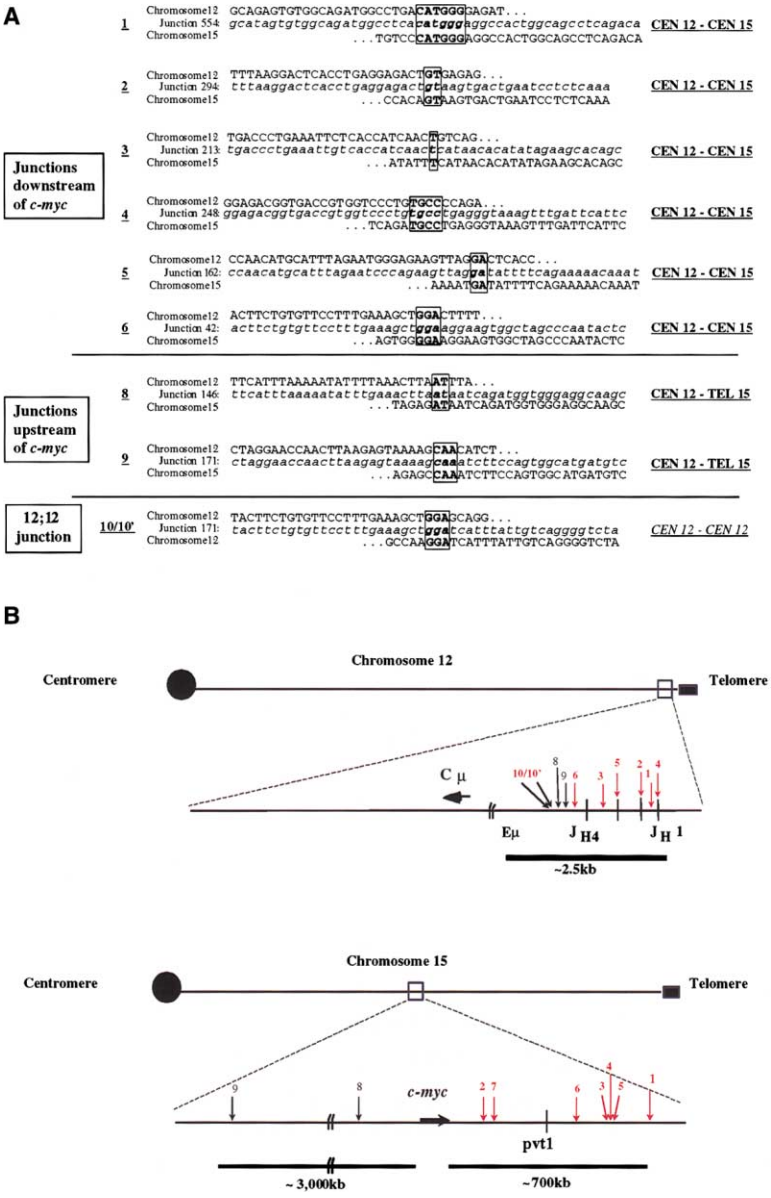

Figure 3. Translocation Junctions Contain Microhomologies and Result in Dicentric Chromosomes

(A) Sequences of cloned translocation junctions are aligned to their corresponding derivative germline sequences. Chromosome 12 sequence is aligned above the junction sequence and chromosome 15 sequence is aligned below. Microhomologies at the junctions are boxed and shown in bold. The configuration of the translocation product is indicated on the right. Junctions that occur downstream of c-*myc* are shown in the first group, junctions that occur upstream of *c-myc* are shown in the second group, and the chromosome 12-12 junction containing divergently fused J_H sequences (tumor #171) is indicated at the bottom.

(B) Map of translocation breakpoints. Each breakpoint is assigned a number corresponding to the alleles described in Table 1. Amplified breakpoints are shown in red. Map is not drawn to scale.

Dicentric Configuration of Amplified Translocation Products

To determine the precise locations of the breaks for each translocation, breakpoint sequences were mapped by comparison to genomic sequence databases (GenBank; Celera CDS). All chromosome 12 breakpoints were clustered in a 2.5 kilobase pair region spanning J_H1 to J_H4, consistent with these breakpoints resulting from a RAG-initiated DSB at a J_H segment. In contrast, breakpoints on chromosome 15 were widely distributed. Six junctions were mapped to positions ranging from 70 kb to more than 700 kb downstream of *c-myc* (Figure 3B, Table 1). Southern blotting demonstrated that each of these downstream junctions was amplified (Figure 1 and see Supplemental Data at http://www.cell.com/cgi/content/full/109/7/811/DC1). While the junctions were spread over an approximately 600 kb region, several clusters were observed, including three junctions within an approximately 2 kb region 372–374 kb downstream of *c-myc* (Figure 3B; see Discussion).

In addition to the six downstream junctions, two junctions were mapped to 134 kb (in tumor #146) and 2700 kb (in tumor #171) upstream of *c-myc* (Figure 3B, Table 1). The upstream junction in 146 was not amplified, and this tumor also lacked an obvious complicon or substantial *c-myc* amplification (see Supplemental Data). This tumor and tumor #184, which has an alteration in the 5′ portion of *c-myc* in the absence of amplification (see above; Gao et al., 2000), may have activated the *c-myc* gene by a different mechanism than the others (see Discussion). Tumor #171 also contained an amplified J_H to J_H junction (Figures 3A and 3B) that likely was generated by mechanisms related to complicon formation (see Discussion). Although tumor #171 contained highly amplified *c-myc* sequences, as well as the amplified J_H to J_H junction (Table 1), its junction 5′ of *c-myc* did not

Table 1. Junction Breakpoints and Amplification

Tumor #	Breakpoint 12	Breakpoint 15	Amplification
554	JH region[1]	705 kb downstream myc[1]	~12-fold
294	JH region[2]	70 kb downstream myc[2]	~11-fold
213	JH region[3]	372 kb downstream myc[3]	~20-fold
248	JH region[4]	373 kb downstream myc[4]	~7-fold
162	JH region[5]	374 kb downstream myc[5]	~10-fold
42[a]	JH region[6]	280 kb downstream myc[6]	~4-fold[b]
127	JH region[c]	~90 kb downstream myc[7]	~9-fold
146[a]	JH region[8]	134 kb upstream myc[8]	NA
171 a	JH region[9]	2711 kb upstream myc[9]	NA[d]
171 b	JH/JH[10/10′]	—	~11-fold

[a] Tumors listed here are either XRCC4 or Lig4, p53 double-deficient, except tumors 42 and 146, which are Lig4, p53, and RAD54 triple-deficient (Essers et al., 1997). These mice developed pro-B lymphoma within 12 weeks of age, indistinguishable from the X/P or L/P mice. A number is assigned to each junction (superscript above), and the map of each numbered junction is shown in Figure 3B. NA, not significantly amplified.

[b] The *c-myc* amplification level was complicated by some DNA degradation in this sample and could be greater than 4-fold.

[c] A 20 kb fragment containing JH sequences was cloned from tumor 127. Limited sequence information indicated that this fragment contains downstream *c-myc* sequences, but the actual junction has not been determined.

[d] Tumor 171 has two junctions, (a) an unamplified rearrangement containing a J_H fused upstream of *c-myc*, and (b) an amplified EcoRI fragment that contains only a JH to JH junction.

appear significantly amplified (data not shown). Notably, chromosome 15-derived sequences adjacent to the 5′ of *c-myc* junction in 171 were amplified in their germline configuration in tumor 171, as well as in several other tumors that contained amplified downstream junctions (data not shown). This finding is consistent with the presence of a large amplicon beginning downstream of *c-myc* and extending at least 3 Mb upstream of *c-myc*. These findings also indicate that the unamplified junction 5′ of *c-myc* in tumor #171 likely resulted from an independent translocation event from that which led to amplified *c-myc*.

The orientation of the translocation junction sequences with respect to the centromeres of the derivative chromosomes demonstrates that all junctions downstream of *c-myc* occurred in a centromere-to-centromere (CEN12-CEN15) configuration, such that the initial translocation product would have resulted in a dicentric chromosome, C12;15C. By contrast, the two unamplified translocation junctions (in tumors #146 and #171) upstream of *c- myc* occurred in a centromere-to-telomere (CEN12-TEL15) configuration, with the centromere of chromosome 12 acquiring chromosome 15 sequence distal to the breakpoint (Figures 3A and 3B), and would have generated C12;15 translocations.

Identification of Dicentric Chromosomes as Intermediates in the Amplification Process

To generate additional tumors to assay for early events in the amplification process, we transferred newborn livers of L/P mice to RAG-deficient recipients. In one transfer, three tumors with amplified *c-myc* genes were generated, two clonally related by J_H rearrangements and one that was distinct (see Supplemental Data at http://www.cell.com/cgi/content/full/109/7/811/DC1).

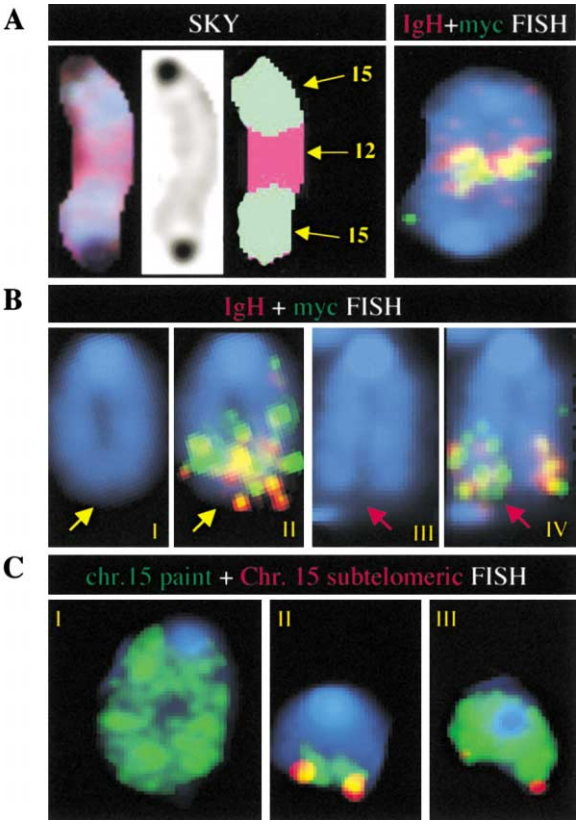

Figure 4. Gene Amplification Process in Action: Fusion of Chromatid Ends and Dicentric Chromosomes

(A) SKY and FISH analyses of a dicentric chromosome in tumor R3. For SKY classification, chromosome 12 and 15 material are indicated. For FISH: the IgH, red; c-*myc*, green; overlap, yellow. DNA is counterstained with DAPI (blue).

(B) FISH analysis of metaphase chromosomes from tumor R3 showing sister chromatid fusions (panels I and II) versus unfused chromatids (panels III and IV). For each set, DAPI-stained chromosomes are at left, FISH signals are displayed at right. Fused chromatids are indicated by yellow arrows and unfused chromatids by red arrows.

(C) FISH analysis of metaphase chromosomes from tumor R3. Chromosome 15-specific paint is displayed in green, and a FISH probe recognizing the near-telomeric region of chromosome 15 is displayed in red. Panel I: chromosome 15 with fused chromatids showing no detectable telomere FISH signal. Panel II: C12;15 translocation with chromosome 15 material and the near-telomeric FISH signal. Panel III: Normal chromosome 15.

Further analyses of these tumors by SKY allowed us to directly visualize rare dicentric translocation products from one tumor (R3). SKY indicated that this dicentric chromosome was symmetric, containing chromosome 12 material between large regions derived from chromosome 15 including centromeres (Figure 4A). FISH showed the coamplification of IgH and *c-myc* on these dicentric chromosomes (Figure 4A). Strikingly, some metaphase chromosomes from this tumor contained a single chromosome possessing sister chromatids fused at their ends. FISH again revealed coamplification of IgH and *c-myc* coincident with sister chromatid fusion (Figure 4B, images I and II) and a lack of chromosome 15 sequences near the telomere, which were present in the C12:15 and normal chromosome 15 in these meta-

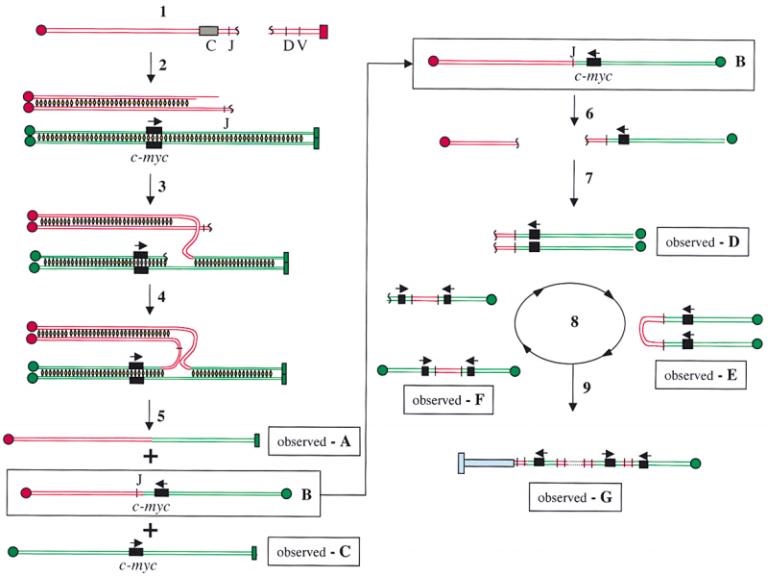

Figure 5. Model for Gene Amplification and Complex Chromosome Translocations in the NHEJ/53-Deficient Lymphomas

Double lines represent chromatids. Chromosome 12 is depicted in red and chromosome 15 in green. At the ends of the chromatids, circles represent centromeres and rectangles represent telomeres. Black symbols situated between chromatids depict sister chromatid cohesion complexes. The blue bars shown for product G indicate material from a third, nonhomologous chromosome. See Discussion for details.

phases (Figure 4C). Finally, we also observed similar chromosomes with amplified IgH and *c-myc* sequences at unfused tips (Figure 4B, images III and IV), consistent with broken dicentrics. These unique chromosomal structures are likely BFB amplification intermediates that are unstable and ultimately give rise to the complicons of more mature tumors.

Discussion

Many types of human tumors contain complex translocations with associated amplifications (complicons). Cell culture studies showed specific DSBs can lead to translocations (Richardson and Jasin, 2000b) or intrachromosomal drug resistance gene amplification (Pipiras et al., 1998). Likewise, such studies implicated p53 in suppression of drug resistance gene amplification (Livingstone et al., 1992; Yin et al., 1992). In this report, we have now linked all of these processes in the setting of tumorigenesis. Thus, in p53-deficient pro-B cells, RAG-initiated DSBs that cannot be repaired by NHEJ inevitably lead to evolution of amplified *c-myc* complicons and, ultimately, to pro-B cell lymphomas.

We have elucidated several features of X/P or L/P lymphomas, which form the basis for a model of oncogenic complicon formation (Figure 5). These include: requirement for a functional RAG2 gene for their generation; presence of a C12;15 nonreciprocal translocation product, which lacks *c-myc* or J_H-proximal IgH sequences; coamplification of IgH and *c-myc* sequences within a complicon and not within the C12;15; occurrence of amplified chromosome 12 to chromosome 15 junctions downstream of *c-myc* in a dicentric orientation; presence of chromosomal intermediates relevant to amplification, including a dicentric C15;12C with amplified *c-myc* and IgH sequences; and generation of translocation junctions by an end-joining pathway that uses short homologies. Although the universal C12;15 in X/P and L/P lymphomas appeared potentially analogous to the classic t(8;14), which harbors fused IgH and *c-myc* loci, of human Burkitt's lymphomas, we now show that it is clearly different. Moreover, the detailed features of X/P or L/P pro-B lymphomas indicate that they are likely more revealing of processes (see below) involved in generation and progression of human solid tumors (Schwab, 1999).

Unrepaired RAG-Initiated DNA Breaks in X/P or L/P Pro-B Cells Lead to C12;15 and C15;12C Translocations

The p53-dependent cell cycle checkpoint responds to DNA damage by inducing cell cycle arrest and/or activating apoptotic programs (Lane, 1992). In XRCC4- or Lig4-deficient mice, the prolymphocyte pool is small, as most likely die from a p53-dependent response to unrepaired RAG-initiated J_H DSBs (Frank et al., 2000; Gao et al., 2000). In X/P or L/P mice, the pro-B compartment size is restored but development is still blocked as RAG-liberated V, (D), and J ends cannot be properly joined without NHEJ (Frank et al., 2000; Gao et al., 2000). This substantial X/P or L/P pro-B cell population with unrepaired Rag-induced DSBs provides a reservoir of cells poised for initiating translocations that lead to transformation. In this context, pro-B cells have been shown to actively cycle in the absence of productive IgH rearrangements (Kline et al., 2001). While the pro-T cell population should similarly be at risk in X/P or L/P mice, absence of X/P or L/P pro-T lymphomas suggests that initiating events are more rare in pro-T cells and/or that potential selective advantages conferred are weaker. A study of CAD gene amplification in a p53-expressing line with a defective G1 checkpoint suggested that checkpoint defects may allow cells to inappropriately move into S phase and subsequently acquire DSBs that initiate amplification (Paulson et al., 1998). RAG-induced DSBs that initiate complicon formation in X/P or L/P pro-B cells occur in G1 or G0 (Lee and Desiderio, 1999). In this context, our findings of chromosome 12 sequences in two different translocations within each tumor and of amplified J_H sequences fused in inverted

orientation in one may be relevant. Together, they imply that X/P- or L/P-deficient pro-B cells with RAG-initiated J_H DSBs cycle into S phase where the DSBs are replicated and ultimately initiate downstream transformation events (Figure 5, steps 1 and 2).

Initiation of Complicon Formation: Linked C12;15 and C15;12C Events

A remarkable feature of X/P or L/P pro-B lymphomas is that they usually harbor both a C12;15 as well as a complicon resulting from a C15;12C dicentric. We have not identified the C12;15 junction. However, it is distinct from amplified junctions, as it usually lacks chromosome 12 sequences proximal to the J_H region (rendering isolation difficult), and involves a more classic C12;15 union with respect to orientation. The C12;15 and the C15;12C might result from separate events, with the C12;15 also selected based on an unknown growth advantage. However, this coincidence may be better explained by mechanistic linkage of C15;12C and C12;15 formation. In the latter scenario, RAG-initiated DSBs in X/P or L/P prolymphocytes would be replicated to yield sister chromatids terminated with IgH locus DSBs held in close proximity due to sister chromatid cohesion established during replication (Figure 5, step 2; reviewed in Carson and Christman, 2001). Because the lagging strand cannot replicate to a broken end, a significant 3′ overhang may result on one sister chromatid, which could become linked to chromosome 15 to yield the observed C12;15 lacking *c-myc* and J_H sequences (Figure 5, step 3; product A). The remaining broken chromatid of 12 could then recombine to the other portion of chromosome 15 to yield the dicentric chromosome (Figure 5, step 4; product B). Directionality of these recombination events might have a mechanistic basis (Richardson and Jasin, 2000a), but in any case would be insured by selection for the dicentric (see below).

The recombination process that generates the C12;15 could be homology mediated or occur via another pathway distinct from NHEJ. One conceivable initiating mechanism would be occurrence of independent DSBs on chromosome 15, for example due to fragile sites (Debatisse et al., 1998). Alternatively, the potential 3′ overhang on one replicated IgH locus DSB could provide a leading strand for a homology-based recombination event; this could leave a DSB on the remaining portion of chromosome 15, as a replication byproduct, that could be coupled to the remaining J_H by end joining. In this context, there is experimental precedent for coupled HR/end-joining recombination events (Richardson and Jasin, 2000a). In any case, ligation of the chromosome 12 and chromosome 15 ends to generate dicentrics clearly involves an end-joining pathway that employs short homologies, perhaps facilitated by proximity of complexed chromosome 12 and 15 ends. In the latter context, microhomology-mediated end joining has recently been characterized as a genetically distinct DNA repair pathway (Verkaik et al., 2002) and is observable in NHEJ-deficient yeast cells and murine cell lines (Roth and Wilson, 1986; Boulton and Jackson, 1996a, 1996b; Kabotyanski et al., 1998). Furthermore, this microhomology-mediated pathway catalyzes aberrant V(D)J coding and signal joining in NHEJ-deficient cells (Bogue et al., 1997; Li et al., 1995; Taccioli et al., 1993). Finally, in vitro studies have also implicated an alternative end-joining pathway (Baumann and West, 1998).

Complicons Are Generated by BFB Cycles from a C15;12C Dicentric

Most human lymphoid malignancies and murine plasmacytomas have IgH and *c-myc* translocations with breakpoints upstream or within *c-myc*, likely activating it via activities of IgH enhancers without amplification (Kuehl and Bergsagel, 2002). Although infrequent compared to amplification, we observed similar events in two lymphomas (#146 and #184; Gao et al., 2000; see Supplemental Data at http://www.cell.com/cgi/content/full/109/7/811/DC1). In contrast, all amplified translocation breakpoints in X/P or L/P lymphomas occur 70 to 700 kb downstream of *c-myc* on chromosome 15. Infrequent translocation junctions in human tumors involving IgL loci occur downstream of *c-myc* but do not result in dicentrics due to the relative orientation of IgL and *c-myc* loci. These junctions suggested potential involvement of downstream sequences, most notably the *plasmacytoma variable translocation-1* (*pvt-1*), which resides about 200 kb downstream (Cory et al., 1985). However, our junctions are more widespread (occurring over an approximately 600 kb region), with some separating *c-myc* from *pvt-1*. As *c-myc* overexpression is a universal feature of all X/P or L/P lymphomas assayed, the location of complicon-initiating translocations downstream of *c-myc* is likely selected based on an efficient mechanism for *c-myc* overexpression via amplification. However, we do not exclude additional roles of ectopic elements such as the 3′IgHRR, given the long-range activity of this putative LCR (reviewed in Manis et al., 2002) and our finding that it is coamplified in the complicons. Finally, we note significant clustering of individual amplified junctions on chromosome 15, most notably three junctions within 372 to 374 kb downstream of *c-myc*. Thus, these junctions are likely targeted by some mechanistic feature, for example potential fragile sites, localized homologies potentially used to generate the C12;15 lesion, or a higher order process that promotes accessibility or proximity (Djalali et al., 1987).

Classic BFB cycles (McClintock, 1941) following dicentric formation are a common mechanism for intrachromosomal gene amplification in drug-resistant mammalian cells (reviewed in Stark, 1993). In this context, we observed predicted dicentric C15;12C (Figure 5, product B) and other intermediates (Figure 5, products D–F) harboring amplified IgH and *c-myc* sequences in L/P tumor cells. Together, these observations suggest the sole requirement for oncogenic *c-myc* amplification in X/P or L/P cells is a C15;12C with the junction falling downstream of *c-myc*. In the absence of p53, a single such initiating event could be amplified rapidly and inevitably by successive BFB cycles (Figure 5, step 8). Ultimately, amplified, unstable chromosomes can be healed by recombination with the telomere-containing region of a separate chromosome (e.g., chromosomes 3 and 6) (Figure 5, step 9, product G). In X/P or L/P lymphomas, the greatly increased frequency of *c-myc* amplification versus ectopic activation of unamplified *c-myc* indicate that overall events leading to amplification are more

frequent than those leading to ectopic activation. In addition, our finding of an inverted amplified J_H to J_H fusion suggests a related, alternative route to complicon formation. In this case, sister chromatids harboring replicated J_H DSBs would be fused to each other, via the alternative end-joining pathway, go through a BFB cycle, and then initiate *c-myc* complicon formation as above but from a different broken chromosome 12 end generated via the first BFB cycle.

General Implications of Complicon Formation in X/P and L/P Pro-B Lymphomas

We have demonstrated several general features of complicon formation in NHEJ/p53-deficient cells. First, the initiating dicentric translocation results from a DSB that is repaired via an end-joining pathway, which is independent of classic NHEJ and HR and employs microhomologies at the junctions. In addition, sister chromatid fusion during BFB cycles appears to occur efficiently in the absence of NHEJ, implying that other pathways play a major role, with some evidence implicating the microhomology-based pathway (e.g., the J_H-J_H fusion). In any case, this poorly understood end-joining pathway represents an important area of future study in the context of genomic stability and tumorigenesis. We further note that complicons are associated with multiple stages of tumor progression (Kuehl and Bergsagel, 2002; Schwab, 1999). For example, in breast cancer, complicon formation involving the c-erbB-2 gene has been implicated in progression from in situ lesions to overt carcinoma (Coene et al., 1997). Most tumors are compromised for cell cycle checkpoints, often due to p53 deficiency. Moreover, even haploinsufficiency for Lig4 in an Ink4a/Arf null background resulted in increased rates of solid tumors (Sharpless et al., 2001). Overall, our findings suggest that complicon formation may be common in many checkpoint-deficient tumors secondary to deficient or insufficient DSBR.

Experimental Procedures

Generation of Complex Mouse Genotypes

Lig IV$^{+/-}$ (Frank et al., 1998) or XRCC4$^{+/-}$ mice (Gao et al., 1998) were bred with p53-deficient mice (Donehower et al., 1992) to generate doubly deficient mice. XRCC4$^{+/-}$, p53$^{+/-}$ mice were also bred with RAG2$^{-/-}$ (Shinkai et al., 1992) mice to generate triple mutant mice. Genotyping of these mutants was performed by PCR or Southern blot analysis of tail DNA as described in the relevant references. Mice were in a mixed 129/C57BL/6 background.

Southern and Northern Analyses

Genomic DNA was isolated from tumor masses or normal tissues from control mice, and Southern blotting was performed as previously described (Frank et al., 2000). RNA samples were extracted from tumor masses or normal tissues from control mice using TriPure Isolation Reagent (Roche). Northern blotting was performed via a standard protocol (Sambrook et al., 1989). Probes for *c-myc* were two Xba fragments from exon 1 and exon 2. A 1.3 kb Pst-1 fragment from the GAPDH gene was used for loading control.

Array CGH

Array CGH analyses were performed by Spectral Genomics (Houston, TX). DNA was prepared according to the recommended Spectral Genomics protocol.

SKY and FISH Analyses

Lymphoma cultures were grown overnight in the presence of 25 ng/ml of IL7 and exposed to 50 ng/ml of colcemid (GIBCO-BRL, KaryoMAX Colecemid solution) for 3–12 hr. Preparation of metaphase chromosomes, SKY analyses, flourescence in situ hybridization (FISH), and whole-chromosome painting using single-chromosome-specific paints were performed as previously described (Sharpless et al., 2001). FISH probes were as follows: *c-myc*, a 20 kb *EcoR*I fragment subcloned into pBluescript spanning the genomic locus; IgH, a plasmid containing the Sγ1 through Cγ1 regions of the IgH locus, as previously described (Skok et al., 2001); J_H region of the IgH locus, a 6 kb *EcoR*I fragment subcloned into pBluescript containing J_H1–J_H4 and Eμ. A BAC from the distal near-telomeric region of mouse chromosome 15 was obtained from Research Genetics.

Cloning and Sequencing of Translocation Junctions

Tumor DNA samples were digested to completion with *EcoR*I, and fragments were cloned into either lambda ZAP II vector (Stratagene) or lambda DASH II vector (Stratagene). Libraries were screened according to standard protocols (Stratagene) using a 2.0 kb *BamHI-EcoRI* fragment derived from the JH-specific FISH probe described above as a probe. Single plaques were purified, subcloned, and sequenced. In the case of lambda ZAPII clones, the inserts were excised according to the protocol provided (Stratagene). Positive clones were verified by restriction analysis and hybridization. Sequencing of subcloned inserts was performed by a core facility using T7 or T3 primers. To obtain junctional sequences, an internal J_H primer was required for some tumors: KMO123, 5′-GGACTTTT CAGGCTCCACCAGACC-3′. As an alternative strategy, a circular PCR protocol was used for cloning and sequencing the junction breakpoints (Megonigal et al., 1998). Briefly, after *EcoR*I digestion, fragments were circularized by dilution and overnight ligation. Ligation reactions were used directly as PCR templates. Appropriately sized PCR products were subcloned into the TOPO cloning vector (Invitrogen), and screened using a J_H probe (Gao et al., 2000). Colonies that positively hybridized with the J_H probe were then purified, and plasmid DNA was isolated and sequenced as described above. Primers for circular PCR were CZO1, 5′-GTTGAGGATTCAGCCGA AACTGGAGAG-3′ and CZO2, 5′-CTTACCTGAGGAGACGGTGACT GAG-3′.

Adoptive Transfer Experiments

Liver cells were collected from neonatal mice and stored on ice while DNA samples were extracted and used for genotyping by PCR. Lig4, p53 double mutant cells were transplanted into four 8- to 12-week-old RAG2-deficient male mice. Recipient mice were irradiated with 200 rad before injection, and 2 million liver cells were transferred to each recipient. Recipient mice were sacrificed 8 weeks after injection when tumor masses were apparent. Tumor samples were collected and analyzed as described above.

Acknowledgments

We thank Craig Bassing and JoAnn Sekiguchi for critical reading of the manuscript. This work was supported by National Institutes of Health grants CA92625 and AI35714 (to F.W.A.). D.O.F. is supported by NIH K08 HL67580-02. K.D.M. is a fellow of the Cure for Lymphoma Foundation, and C.Z. was a fellow of the Cancer Research Institute. C.L. is a Stanley Robbins Award recipient. F.W.A. is an investigator, and C.Z. and K.D.M. were associates of the Howard Hughes Medical Institute.

Received: April 25, 2002
Revised: May 24, 2002
Published online: May 29, 2002

References

Alt, F.W., Kellems, R.E., Bertino, J.R., and Schimke, R.T. (1978). Selective multiplication of dihydrofolate reductase genes in methotrexate-resistant variants of cultured murine cells. J. Biol. Chem. *253*, 1357–1370.

Bassing, C.H., Swat, W., and Alt, F.W. (2002). The mechanism and regulation of chromosomal V(D)J recombination. Cell *109*, S45–S55.

Baumann, P., and West, S.C. (1998). DNA end-joining catalyzed by human cell-free extracts. Proc. Natl. Acad. Sci. USA *95*, 14066–14070.

Bogue, M.A., Wang, C., Zhu, C., and Roth, D.B. (1997). V(D)J recombination in Ku86-deficient mice: distinct effects on coding, signal, and hybrid joint formation. Immunity *7*, 37–47.

Boulton, S.J., and Jackson, S.P. (1996a). Identification of a *Saccharomyces cerevisiae* Ku80 homologue: roles in DNA double-strand break rejoining and in telomeric maintenance. Nucleic Acids Res. *24*, 4639–4648.

Boulton, S.J., and Jackson, S.P. (1996b). *Saccharomyces cerevisiae* Ku70 potentiates illegitimate DNA double-strand break repair and serves as a barrier to error-prone DNA repair pathways. EMBO J. *15*, 5093–5103.

Carson, D.R., and Christman, M.F. (2001). Evidence that replication fork components catalyze establishment of cohesion between sister chromatids. Proc. Natl. Acad. Sci. USA *98*, 8270–8275.

Coene, E.D., Schelfhout, V., Winkler, R.A., Schelfhout, A.M., Van Roy, N., Grooteclaes, M., Speleman, F., and De Potter, C.R. (1997). Amplification units and translocation at chromosome 17q and c-erbB-2 overexpression in the pathogenesis of breast cancer. Virchows Arch. *430*, 365–372.

Coquelle, A., Pipiras, E., Toledo, F., Buttin, G., and Debatisse, M. (1997). Expression of fragile sites triggers intrachromosomal mammalian gene amplification and sets boundaries to early amplicons. Cell *89*, 215–225.

Cory, S., Graham, M., Webb, E., Corcoran, L., and Adams, J.M. (1985). Variant (6;15) translocations in murine plasmacytomas involve a chromosome 15 locus at least 72 kb from the c-myc oncogene. EMBO J. *4*, 675–681.

Debatisse, M., Coquelle, A., Toledo, F., and Buttin, G. (1998). Gene amplification mechanisms: the role of fragile sites. Recent Results Cancer Res. *154*, 216–226.

Difilippantonio, M.J., Zhu, J., Chen, H.T., Meffre, E., Nussenzweig, M.C., Max, E.E., Ried, T., and Nussenzweig, A. (2000). DNA repair protein Ku80 suppresses chromosomal aberrations and malignant transformation. Nature *404*, 510–514.

Djalali, M., Adolph, S., Steinbach, P., Winking, H., and Hameister, H. (1987). A comparative mapping study of fragile sites in the human and murine genomes. Hum. Genet. *77*, 157–162.

Donehower, L.A., Harvey, M., Slagle, B.L., McArthur, M.J., Montgomery, C.A., Jr., Butel, J.S., and Bradley, A. (1992). Mice deficient for p53 are developmentally normal but susceptible to spontaneous tumours. Nature *356*, 215–221.

Essers, J., Hendriks, R.W., Swagemakers, S.M., Troelstra, C, de Wit, J., Bootsma, D., Hoeijmakers, J.H., and Kanaar, R. (1997). Disruption of mouse RAD54 reduces ionizing radiation resistance and homologous recombination. Cell *89*, 195–204.

Federspiel, N.A., Beverley, S.M., Schilling, J.W., and Schimke, R.T. (1984). Novel DNA rearrangements are associated with dihydrofolate reductase gene amplification. J. Biol. Chem. *259*, 9127–9140.

Ferguson, D.O., and Alt, F.W. (2001). DNA double-strand break repair and chromosomal translocation: lessons from animal models. Oncogene *20*, 5572–5579.

Frank, K.M., Sekiguchi, J.M., Seidl, K.J., Swat, W., Rathbun, G.A., Cheng, H.L., Davidson, L., Kangaloo, L., and Alt, F.W. (1998). Late embryonic lethality and impaired V(D)J recombination in mice lacking DNA ligase IV. Nature *396*, 173–177.

Frank, K.M., Sharpless, N.E., Gao, Y., Sekiguchi, J.M., Ferguson, D.O., Zhu, C., Manis, J.P., Horner, J., DePinho, R.A., and Alt, F.W. (2000). DNA ligase IV deficiency in mice leads to defective neurogenesis and embryonic lethality via the p53 pathway. Mol. Cell *5*, 993–1002.

Fugmann, S.D., Lee, A.I., Shockett, P.E., Villey, I.J., and Schatz, D.G. (2000). The RAG proteins and V(D)J recombination: complexes, ends, and transposition. Annu. Rev. Immunol. *18*, 495–527.

Gao, Y., Sun, Y., Frank, K.M., Dikkes, P., Fujiwara, Y., Seidl, K.J., Sekiguchi, J.M., Rathbun, G.A., Swat, W., Wang, J., et al. (1998). A critical role for DNA end-joining proteins in both lymphogenesis and neurogenesis. Cell *95*, 891–902.

Gao, Y., Ferguson, D.O., Xie, W., Manis, J., Sekiguchi, J., Frank, K.M., Chaudhuri, J., Horner, J., DePinho, R.A., and Alt, F.W. (2000). Interplay of p53 and DNA-repair protein XRCC4 in tumorigenesis, genomic stability and development. Nature *404*, 897–900.

Gorre, M.E., Mohammed, M., Ellwood, K., Hsu, N., Paquette, R., Rao, P.N., and Sawyers, C.L. (2001). Clinical resistance to STI-571 cancer therapy caused by BCR-ABL gene mutation or amplification. Science *293*, 876–880.

Gu, Y., Seidl, K.J., Rathbun, G.A., Zhu, C., Manis, J.P., van der Stoep, N., Davidson, L., Cheng, H.L., Sekiguchi, J.M., Frank, K., et al. (1997). Growth retardation and leaky SCID phenotype of Ku70-deficient mice. Immunity *7*, 653–665.

Kabotyanski, E.B., Gomelsky, L., Han, J.O., Stamato, T.D., and Roth, D.B. (1998). Double-strand break repair in Ku86- and XRCC4-deficient cells. Nucleic Acids Res. *26*, 5333–5342.

Kline, G.H., Hayden, T.A., and Riegert, P. (2001). The initiation of B cell clonal expansion occurs independently of pre-B cell receptor formation. J. Immunol. *167*, 5136–5142.

Kuehl, W.M., and Bergsagel, P.L. (2002). Multiple myeloma: evolving genetic events and host interactions. Nature Rev. Cancer *2*, 175–187.

Kuo, M.T., Vyas, R.C., Jiang, L.X., and Hittelman, W.N. (1994). Chromosome breakage at a major fragile site associated with P-glycoprotein gene amplification in multidrug-resistant CHO cells. Mol. Cell. Biol. *14*, 5202–5211.

Lane, D.P. (1992). Cancer. p53, guardian of the genome. Nature *358*, 15–16.

Lee, J., and Desiderio, S. (1999). Cyclin A/CDK2 regulates V(D)J recombination by coordinating RAG-2 accumulation and DNA repair. Immunity *11*, 771–781.

Lengauer, C., Kinzler, K.W., and Vogelstein, B. (1998). Genetic instabilities in human cancers. Nature *396*, 643–649.

Li, Z., Otevrel, T., Gao, Y., Cheng, H.L., Seed, B., Stamato, T.D., Taccioli, G.E., and Alt, F.W. (1995). The XRCC4 gene encodes a novel protein involved in DNA double-strand break repair and V(D)J recombination. Cell *83*, 1079–1089.

Lim, D.S., Vogel, H., Willerford, D.M., Sands, A.T., Platt, K.A., and Hasty, P. (2000). Analysis of ku80-mutant mice and cells with deficient levels of p53. Mol. Cell. Biol. *20*, 3772–3780.

Livingstone, L.R., White, A., Sprouse, J., Livanos, E., Jacks, T., and Tlsty, T.D. (1992). Altered cell cycle arrest and gene amplification potential accompany loss of wild-type p53. Cell *70*, 923–935.

Liyanage, M., Coleman, A., du Manoir, S., Veldman, T., McCormack, S., Dickson, R.B., Barlow, C., Wynshaw-Boris, A., Janz, S., Wienberg, J., et al. (1996). Multicolour spectral karyotyping of mouse chromosomes. Nat. Genet. *14*, 312–315.

Ma, C., Martin, S., Trask, B., and Hamlin, J.L. (1993). Sister chromatid fusion initiates amplification of the dihydrofolate reductase gene in Chinese hamster cells. Genes Dev. *7*, 605–620.

Manis, J.P., Tian, M., and Alt, F.W. (2002). Mechanism and control of class-switch recombination. Trends Immunol. *23*, 31–39.

McClintock, B. (1941). The stability of broken ends of chromosomes in Zea mays. Genetics *26*, 234–282.

Megonigal, M.D., Rappaport, E.F., Jones, D.H., Williams, T.M., Lovett, B.D., Kelly, K.M., Lerou, P.H., Moulton, T., Budarf, M.L., and Felix, C.A. (1998). t(11;22)(q23;q11.2) in acute myeloid leukemia of infant twins fuses MLL with hCDCrel, a cell division cycle gene in the genomic region of deletion in DiGeorge and velocardiofacial syndromes. Proc. Natl. Acad. Sci. USA *95*, 6413–6418.

Padilla-Nash, H.M., Heselmeyer-Haddad, K., Wangsa, D., Zhang, H., Ghadimi, B.M., Macville, M., Augustus, M., Schrock, E., Hilgenfeld, E., and Ried, T. (2001). Jumping translocations are common in solid tumor cell lines and result in recurrent fusions of whole chromosome arms. Genes Chromosomes Cancer *30*, 349–363.

Paulson, T.G., Almasan, A., Brody, L.L., and Wahl, G.M. (1998). Gene amplification in a p53-deficient cell line requires cell cycle progres-

sion under conditions that generate DNA breakage. Mol. Cell. Biol. *18*, 3089–3100.

Pinkel, D., Segraves, R., Sudar, D., Clark, S., Poole, I., Kowbel, D., Collins, C., Kuo, W.L., Chen, C., Zhai, Y., et al. (1998). High resolution analysis of DNA copy number variation using comparative genomic hybridization to microarrays. Nat. Genet. *20*, 207–211.

Pipiras, E., Coquelle, A., Bieth, A., and Debatisse, M. (1998). Interstitial deletions and intrachromosomal amplification initiated from a double-strand break targeted to a mammalian chromosome. EMBO J. *17*, 325–333.

Richardson, C., and Jasin, M. (2000a). Coupled homologous and nonhomologous repair of a double-strand break preserves genomic integrity in mammalian cells. Mol. Cell. Biol. *20*, 9068–9075.

Richardson, C., and Jasin, M. (2000b). Frequent chromosomal translocations induced by DNA double-strand breaks. Nature *405*, 697–700.

Roth, D.B., and Wilson, J.H. (1986). Nonhomologous recombination in mammalian cells: role for short sequence homologies in the joining reaction. Mol. Cell. Biol. *6*, 4295–4304.

Sambrook, J., Fritsch, E.F., and Maniatis, T. (1989). Molecular Cloning: A Laboratory Manual, 2nd ed. (Cold Spring Harbor, NY: Cold Spring Harbor Laboratory Press).

Schwab, M. (1999). Oncogene amplification in solid tumors. Semin. Cancer Biol. *9*, 319–325.

Sharpless, N.E., Ferguson, D.O., O'Hagan, R.C., Castrillon, D.H., Lee, C., Farazi, P.A., Alson, S., Fleming, J., Morton, C.C., Frank, K., et al. (2001). Impaired nonhomologous end-joining provokes soft tissue sarcomas harboring chromosomal translocations, amplifications, and deletions. Mol. Cell *8*, 1187–1196.

Shinkai, Y., Rathbun, G., Lam, K.P., Oltz, E.M., Stewart, V., Mendelsohn, M., Charron, J., Datta, M., Young, F., Stall, A.M., et al. (1992). RAG-2-deficient mice lack mature lymphocytes owing to inability to initiate V(D)J rearrangement. Cell *68*, 855–867.

Skok, J.A., Brown, K.E., Azuara, V., Caparros, M.L., Baxter, J., Takacs, K., Dillon, N., Gray, D., Perry, R.P., Merkenschlager, M., and Fisher, A.G. (2001). Nonequivalent nuclear location of immunoglobulin alleles in B lymphocytes. Nat. Immunol. *2*, 848–854.

Smith, K.A., Gorman, P.A., Stark, M.B., Groves, R.P., and Stark, G.R. (1990). Distinctive chromosomal structures are formed very early in the amplification of CAD genes in Syrian hamster cells. Cell *63*, 1219–1227.

Stark, G.R. (1993). Regulation and mechanisms of mammalian gene amplification. Adv. Cancer Res. *61*, 87–113.

Taccioli, G.E., Rathbun, G., Oltz, E., Stamato, T., Jeggo, P.A., and Alt, F.W. (1993). Impairment of V(D)J recombination in double-strand break repair mutants. Science *260*, 207–210.

Toledo, F., Le Roscouet, D., Buttin, G., and Debatisse, M. (1992). Co-amplified markers alternate in megabase long chromosomal inverted repeats and cluster independently in interphase nuclei at early steps of mammalian gene amplification. EMBO J. *11*, 2665–2673.

Vanasse, G.J., Halbrook, J., Thomas, S., Burgess, A., Hoekstra, M.F., Disteche, C.M., and Willerford, D.M. (1999). Genetic pathway to recurrent chromosome translocations in murine lymphoma involves V(D)J recombinase. J. Clin. Invest. *103*, 1669–1675.

Verkaik, N.S., Esveldt-van Lange, R.E., van Heemst, D., Bruggenwirth, H.T., Hoeijmakers, J.H., Zdzienicka, M.Z., and van Gent, D.C. (2002). Different types of V(D)J recombination and end-joining defects in DNA double-strand break repair mutant mammalian cells. Eur. J. Immunol. *32*, 701–709.

Windle, B., Draper, B.W., Yin, Y.X., O'Gorman, S., and Wahl, G.M. (1991). A central role for chromosome breakage in gene amplification, deletion formation, and amplicon integration. Genes Dev. *5*, 160–174.

Yin, Y., Tainsky, M.A., Bischoff, F.Z., Strong, L.C., and Wahl, G.M. (1992). Wild-type p53 restores cell cycle control and inhibits gene amplification in cells with mutant p53 alleles. Cell *70*, 937–948.

Zimmerman, K., and Alt, F.W. (1990). Expression and function of myc family genes. Crit. Rev. Oncog. *2*, 75–95.